

Analysis of $B \rightarrow a_1(1260)(b_1(1235))K^*$ decays in the perturbative QCD approach^{*}

ZHANG Zhi-Qing(张志清)¹⁾ FU Jian-Hua(符建华)

Department of Physics, Henan University of Technology, Zhengzhou 450001, China

Abstract: Within the framework of the perturbative quantum chromodynamics (PQCD) approach, we study the charmless two-body decays $B \rightarrow a_1(1260)K^*$, $b_1(1235)K^*$. Using the decay constants and the light-cone distribution amplitudes for these mesons derived from the QCD sum rule method, we find the following results. (a) Our predictions for the branching ratios are consistent with the QCD factorization (QCDF) results within errors, but much larger than the naive factorization approach calculation values. (b) We predict that the anomalous polarizations occurring in the decays $B \rightarrow \phi K^*$, ρK^* also happen in $B \rightarrow a_1 K^*$ decays, while they do not happen in $B \rightarrow b_1 K^*$ decays. Here the contributions from the annihilation diagrams play an important role in explaining the larger transverse polarizations in the $B \rightarrow a_1 K^*$ decays, while they are not sensitive to the polarizations for the $B \rightarrow b_1 K^*$ decays. (c) Our predictions for the direct CP -asymmetries agree well with the QCDF results within errors. The decays $\bar{B}^0 \rightarrow b_1^+ K^{*-}$, $B^- \rightarrow b_1^0 K^{*-}$ have larger direct CP -asymmetries, which could be measured by the present LHCb experiment and the forthcoming Super-B experiment.

Key words: PQCD approach, B meson decay, polarization

PACS: 13.25.Hw, 12.38.Bx, 14.40.Nd **DOI:** 10.1088/1674-1137/39/3/033102

1 Introduction

In general, mesons are classified in J^{PC} multiplets. There are two types of orbitally excited axial-vector mesons, namely, 1^{++} and 1^{+-} . The former includes $a_1(1260)$, $f_1(1285)$, $f_1(1420)$, and K_{1A} , which compose the 3P_1 nonet; the latter includes $b_1(1235)$, $h_1(1170)$, $h_1(1380)$, and K_{1B} , which compose the 1P_1 nonet. With the exception of $a_1(1260)$ and $b_1(1235)$, these axial-vector mesons have an important characteristic: each flavor state can mix with any other flavor state from the other nonet or the same nonet. There is no mixing between $a_1(1260)$ and $b_1(1235)$ because of their opposite C parities. They also do not mix with the other mesons. So, compared with other axial-vector mesons, these two mesons should have less uncertainty regarding their inner structures.

Like the decay modes $B \rightarrow VV$, the charmless decays $B \rightarrow a_1(1260)K^*$, $b_1(1235)K^*$ also have three polarization states and so are expected to have rich physics. In many $B \rightarrow VV$ decays, the information on branching ratios and polarization fractions among various he-

licity amplitudes have been studied by many authors [1–4]. Through polarization studies, some underlying helicity structure in the decay mechanism is suggested. It has been found that the polarization fractions follow the naive counting rule, that is $f_L \sim 1 - O(m_V^2/m_B^2)$, $f_N \sim f_T \sim O(m_V^2/m_B^2)$, where $f_{L,N,T}$ denote the longitudinal, parallel, and perpendicular polarization fractions, respectively, and $m_B(m_V)$ is the $B(V)$ meson mass. If the contributions from the factorizable emission amplitudes are suppressed for some decay modes, however, this counting rule might be modified dramatically by other contributions. For example, highly anomalous longitudinal polarization fractions of about 50% have been measured in the decays $B \rightarrow \rho K^*$, ϕK^* [5], apart from the decay $B^- \rightarrow K^{*-} \rho^0$, which has a large longitudinal polarization fraction of $(96_{-16}^{+6})\%$ [5] (the newer measurement is $(90 \pm 20)\%$ [6]). Whether similar results also occur in the decay modes $B \rightarrow a_1(1260)K^*$, $b_1(1235)K^*$ is worth researching. We know that $a_1(1260)$ has some similar behaviors to the vector meson, so one can expect the branching ratios and polarization fractions of the decays $B \rightarrow a_1(1260)K^*$ and $B \rightarrow \rho K^*$, where $a_1(1260)$ and ρ are

Received 1 April 2014, Revised 14 August 2014

^{*} Supported by National Natural Science Foundation of China (11147004, 11347030), Program of Youthful Key Teachers in University of Henan Province (001166), and by Foundation of Henan Educational Committee (14HASTIT037)

1) E-mail: zhangzhiqing@haut.edu.cn



Content from this work may be used under the terms of the Creative Commons Attribution 3.0 licence. Any further distribution of this work must maintain attribution to the author(s) and the title of the work, journal citation and DOI. Article funded by SCOAP³ and published under licence by Chinese Physical Society and the Institute of High Energy Physics of the Chinese Academy of Sciences and the Institute of Modern Physics of the Chinese Academy of Sciences and IOP Publishing Ltd

scalar partners of each other, to have similar characteristics. This is not the case for $b_1(1235)$ because of the different characteristics of its decay constant and light-cone distribution amplitudes (LCDAs) compared with those of $a_1(1260)$. For example, the longitudinal decay constant is very small for the charged $b_1(1235)$ states and vanishes under the $SU(3)$ limit. It is zero for the neutral $b_1^0(1235)$ state. The transverse decay constant of $a_1(1260)$, on the other hand, vanishes under the $SU(3)$ limit. In the isospin limit, the chiral-odd (-even) LCDAs of the $b_1(1235)$ meson are symmetric (antisymmetric) under the exchange of quark and antiquark momentum fractions, which is exactly opposite to the symmetric behavior for $a_1(1260)$. In view of these differences, one can expect that $B \rightarrow a_1(1260)K^*$ and $B \rightarrow b_1(1235)K^*$ should give very different results. On the theoretical side, the decays $B \rightarrow a_1(1260)K^*$, $b_1(1235)K^*$ have been studied by Cheng and Yang in [7], where the branching ratios are very different to those calculated by the naive factorization approach [8]. To clarify such large differences is another motivation of this work. On the experimental side, only the upper limits for some of the considered decays are available [9, 10].

In the following, $a_1(1260)$ and $b_1(1235)$ are denoted as a_1 and b_1 in some places for convenience. The layout of this paper is as follows. In Section 2, we analyze these decay channels using the perturbative quantum chromodynamics (PQCD) approach. The numerical results and discussion are given in Section 3. The conclusions are presented in the final part.

2 The PQCD calculation

The PQCD approach has proven an effective theory to handle hadronic B decays in many works [2, 3, 11, 12]. Because the transverse momentum of the valence quarks in the hadrons is taken into account, one will encounter double logarithm divergences when the soft and the collinear momenta overlap. Fortunately, these large double logarithms can be re-summed into the Sudakov factor [13]. There is also another type of double logarithm which arises from the loop corrections to the weak decay vertex. These double logarithms can also be re-summed and result in the threshold factor, which decreases faster than any other power of the momentum fraction in the threshold region, which removes the endpoint singularity. This factor is often parameterized into a simple form which is independent of channels, twists and flavors [14]. Certainly, when the higher order diagrams only suffer from soft or collinear infrared divergence, it is easy to cure using the eikonal approximation [15]. Controlling these kinds of divergences reasonably makes the PQCD

approach more self-consistent.

In the standard model, the related weak effective Hamiltonian H_{eff} mediating the $b \rightarrow s$ type transitions can be written as [16]

$$\mathcal{H}_{\text{eff}} = \frac{G_F}{\sqrt{2}} \left[\sum_{p=u,c} V_{pb} V_{ps}^* (C_1(\mu) O_1^p(\mu) + C_2(\mu) O_2^p(\mu)) - V_{tb} V_{ts}^* \sum_{i=3}^{10} C_i(\mu) O_i(\mu) \right]. \quad (1)$$

Here the function $Q_i (i = 1, \dots, 10)$ is the local four-quark operator and C_i is the corresponding Wilson coefficient. $V_{p(t)b}$, $V_{p(t)s}$ are the Cabibbo-Kobayashi-Maskawa (CKM) matrix elements. The standard four-quark operators are defined as:

$$\begin{aligned} O_1^u &= \bar{s}_\alpha \gamma^\mu L u_\beta \cdot \bar{u}_\beta \gamma_\mu L b_\alpha, \\ O_2^u &= \bar{s}_\alpha \gamma^\mu L u_\alpha \cdot \bar{u}_\beta \gamma_\mu L b_\beta, \\ O_3 &= \bar{s}_\alpha \gamma^\mu L b_\alpha \cdot \sum_{q'} \bar{q}'_\beta \gamma_\mu L q'_\beta, \\ O_4 &= \bar{s}_\alpha \gamma^\mu L b_\beta \cdot \sum_{q'} \bar{q}'_\beta \gamma_\mu L q'_\alpha, \\ O_5 &= \bar{s}_\alpha \gamma^\mu L b_\alpha \cdot \sum_{q'} \bar{q}'_\beta \gamma_\mu R q'_\beta, \\ O_6 &= \bar{s}_\alpha \gamma^\mu L b_\beta \cdot \sum_{q'} \bar{q}'_\beta \gamma_\mu R q'_\alpha, \\ O_7 &= \frac{3}{2} \bar{s}_\alpha \gamma^\mu L b_\alpha \cdot \sum_{q'} e_{q'} \bar{q}'_\beta \gamma_\mu R q'_\beta, \\ O_8 &= \frac{3}{2} \bar{s}_\alpha \gamma^\mu L b_\beta \cdot \sum_{q'} e_{q'} \bar{q}'_\beta \gamma_\mu R q'_\alpha, \\ O_9 &= \frac{3}{2} \bar{s}_\alpha \gamma^\mu L b_\alpha \cdot \sum_{q'} e_{q'} \bar{q}'_\beta \gamma_\mu L q'_\beta, \\ O_{10} &= \frac{3}{2} \bar{s}_\alpha \gamma^\mu L b_\beta \cdot \sum_{q'} e_{q'} \bar{q}'_\beta \gamma_\mu L q'_\alpha, \end{aligned} \quad (2)$$

where α and β are the $SU(3)$ color indices; L and R are the left- and right-handed projection operators with $L = (1 - \gamma_5)$, $R = (1 + \gamma_5)$. The sum over q' runs over the quark fields that are active at the scale $\mu = O(m_b)$, i.e. ($q' \in \{u, d, s, c, b\}$). At leading order, there are eight types of single hard gluon exchange diagrams which contribute to the decays we are considering. These can be divided into emission type diagrams and annihilation type diagrams, each type including two factorizable and two non-factorizable diagrams. Due to space limitations, these diagrams are not shown here.

Combining the contributions from the different diagrams, the total decay amplitudes for these decays can be written as

$$\begin{aligned}
 \sqrt{2}\mathcal{M}_j(\bar{K}^{*0}a_1^0) &= \xi_u(F_{eK^*}^{LL,j}a_2+M_{eK^*}^{LL,j}C_2)-\xi_t\left[F_{eK^*}^{LL,j}\left(\frac{3C_7}{2}+\frac{C_8}{2}+\frac{3C_9}{2}+\frac{C_{10}}{2}\right)\right. \\
 &\quad -\left(F_{ea_1}^{LL,j}+F_{aa_1}^{LL,j}\right)\left(a_4-\frac{a_{10}}{2}\right)+M_{eK^*}^{LL,j}\frac{3C_{10}}{2}+M_{eK^*}^{SP,j}\frac{3C_8}{2} \\
 &\quad -\left(M_{ea_1}^{LL,j}+M_{aa_1}^{LL,j}\right)\left(C_3-\frac{1}{2}C_9\right)-\left(M_{ea_1}^{LR,j}+M_{aa_1}^{LR,j}\right)\left(C_5-\frac{1}{2}C_7\right) \\
 &\quad \left.-\left(F_{ea_1}^{SP,j}+F_{aa_1}^{SP,j}\right)\left(a_6-\frac{1}{2}a_8\right)\right], \quad (3)
 \end{aligned}$$

$$\begin{aligned}
 \mathcal{M}_j(\bar{K}^{*0}a_1^-) &= \xi_u\left[M_{aa_1}^{LL,j}C_1+F_{aa_1}^{LL,j}a_1\right]-\xi_t\left[F_{ea_1}^{LL,j}\left(a_4-\frac{a_{10}}{2}\right)+F_{aa_1}^{LL,j}\left(a_4+a_{10}\right)\right. \\
 &\quad +M_{ea_1}^{LL,j}\left(C_3-\frac{1}{2}C_9\right)+M_{aa_1}^{LL,j}\left(C_3+C_9\right)+M_{ea_1}^{LR,j}\left(C_5-\frac{1}{2}C_7\right) \\
 &\quad \left.+M_{aa_1}^{LR,j}\left(C_5+C_7\right)+F_{aa_1}^{SP,j}\left(a_6+a_8\right)\right], \quad (4)
 \end{aligned}$$

$$\begin{aligned}
 \sqrt{2}\mathcal{M}_j(\bar{K}^{*-}a_1^0) &= \xi_u\left[F_{eK^*}^{LL,j}a_2+M_{eK^*}^{LL,j}C_2+M_{aa_1}^{LL,j}C_1+F_{aa_1}^{LL,j}a_1\right]-\xi_t\left[M_{eK^*}^{LL,j}\frac{3}{2}C_{10}\right. \\
 &\quad +M_{eK^*}^{SP,j}\frac{3}{2}C_8+M_{aa_1}^{LL,j}\left(C_3+C_9\right)+M_{aa_1}^{LR,j}\left(C_5+C_7\right) \\
 &\quad \left.+F_{aa_1}^{LL,j}\left(a_4+a_{10}\right)+F_{aa_1}^{SP,j}\left(a_6+a_8\right)\right], \quad (5)
 \end{aligned}$$

$$\begin{aligned}
 \mathcal{M}_j(\bar{K}^{*-}a_1^+) &= \xi_u\left[F_{ea_1}^{LL,j}a_1+M_{ea_1}^{LL,j}C_1\right]-\xi_t\left[F_{ea_1}^{LL,j}\left(a_4+a_{10}\right)+M_{ea_1}^{LL,j}\left(C_3+C_9\right)\right. \\
 &\quad +M_{ea_1}^{LR,j}\left(C_5+C_7\right)+M_{aa_1}^{LL,j}\left(C_3-\frac{1}{2}C_9\right)+M_{aa_1}^{LR,j}\left(C_5-\frac{1}{2}C_7\right) \\
 &\quad \left.+F_{aa_1}^{LL,j}\left(a_4-\frac{1}{2}a_{10}\right)+F_{aa_1}^{SP,j}\left(a_6-\frac{1}{2}a_8\right)\right], \quad (6)
 \end{aligned}$$

where $F_{ea_1}^{LL,j}$ denotes the amplitudes of the factorizable emission diagrams, where one can extract out the $B \rightarrow a_1$ transition form factor. If we exchange the positions of a_1 and \bar{K}^* , we get the amplitudes $F_{eK^*}^{LL,j}$ and $F_{eK^*}^{SP,j}$. As for the amplitudes of the non-factorizable emission diagrams, $M_{ea_1}^{LL,j}$ and $M_{ea_1}^{LR,j}$ are those relevant to the decays considered. The amplitudes $M_{eK^*}^{LL,j}$ and $M_{eK^*}^{SP,j}$ are obtained by exchanging a_1 and \bar{K}^* in the non-factorizable emission diagrams. In a similar way, for the annihilation diagram amplitudes $F_{aa_1}^{LL,j}$ and $F_{aa_1}^{SP,j}$ are from the factorizable annihilation diagrams, while $M_{aa_1}^{LL,j}$ and $M_{aa_1}^{LR,j}$ are from the non-factorizable annihilation diagrams. Note that the upper labels LL, LR, and SP denote the $(V-A)(V-A)$, $(V-A)(V+A)$, and $(S-P)(S+P)$ currents, respectively, and j denotes three types of polarizations (one longitudinal and two transverse), denoted by L , N and T . Limitations of space prevent us from giving the analytical expressions for these amplitudes. The combinations of the Wilson coefficients are defined as usual:

$$a_1(\mu) = C_2(\mu) + \frac{C_1(\mu)}{3}, \quad a_2(\mu) = C_1(\mu) + \frac{C_2(\mu)}{3}, \quad (7)$$

$$a_i(\mu) = C_i(\mu) + \frac{C_{i+1}(\mu)}{3}, \quad i=3,5,7,9, \quad (8)$$

$$a_i(\mu) = C_i(\mu) + \frac{C_{i-1}(\mu)}{3}, \quad i=4,6,8,10. \quad (9)$$

The amplitudes for those decays involving the b_1 meson can be found from Eq. (4)–Eq. (6) above by substituting the b_1 meson wave functions for a_1 ones.

3 Numerical results and discussions

For the wave function of the heavy B meson, we take [11]

$$\Phi_B(x,b) = \frac{1}{\sqrt{2N_c}}(\not{P}_B + m_B)\gamma_5\phi_B(x,b). \quad (10)$$

Here only the contribution of the Lorentz structure $\phi_B(x,b)$ is taken into account, since the contribution of the second Lorentz structure $\tilde{\phi}_B$ is numerically small [17] and has been neglected. For the distribution amplitude $\phi_B(x,b)$ in Eq. (10), we adopt the following model:

$$\phi_B(x,b) = N_B x^2(1-x)^2 \exp\left[-\frac{M_B^2 x^2}{2\omega_b^2} - \frac{1}{2}(\omega_b b)^2\right], \quad (11)$$

where ω_b is a free parameter, taken to be $\omega_b = 0.4 \pm 0.04$ GeV in numerical calculations, and $N_B = 91.745$ is the normalization factor for $\omega_b = 0.4$. This is the same wave function as in Ref. [11], which gives the best fit for most of the measured hadronic B decays.

In these decays, both the longitudinal and the transverse polarizations are involved for the vector meson K^* .

Its distribution amplitudes are defined as

$$\begin{aligned} & \langle K^*(P, \epsilon_L^*) | \bar{q}_{2\beta}(z) q_{1\alpha}(0) | 0 \rangle \\ &= \frac{1}{\sqrt{2N_c}} \int_0^1 dx e^{ixp \cdot z} [m_{K^*} \epsilon_L^* \phi_{K^*}^t(x) + \epsilon_L^* \not{P} \phi_{K^*}^t(x) \\ & \quad + m_{K^*} \phi_{K^*}^s(x)]_{\alpha\beta}, \end{aligned} \quad (12)$$

$$\begin{aligned} & \langle K^*(P, \epsilon_T^*) | \bar{q}_{2\beta}(z) q_{1\alpha}(0) | 0 \rangle \\ &= \frac{1}{\sqrt{2N_c}} \int_0^1 dx e^{ixp \cdot z} [m_{K^*} \epsilon_T^* \phi_{K^*}^v(x) + \epsilon_T^* \not{P} \phi_{K^*}^T(x) \\ & \quad + m_{K^*} i \epsilon_{\mu\nu\rho\sigma} \gamma_5 \gamma^\mu \epsilon_T^{*\nu} n^\rho v^\sigma \phi_{K^*}^a(x)]_{\alpha\beta}, \end{aligned} \quad (13)$$

where $n(v)$ is the unit vector having the same (opposite) direction as the motion of the vector meson and x is the momentum fraction of quark q_2 . The upper (sub)leading twist wave functions can be parameterized as

$$\begin{aligned} \phi_{K^*}(x) &= \frac{f_{K^*}}{2\sqrt{2N_c}} \phi_{\parallel}(x), \phi_{K^*}^T(x) = \frac{f_{K^*}^T}{2\sqrt{2N_c}} \phi_{\perp}(x), \\ \phi_{K^*}^t(x) &= \frac{f_{K^*}^T}{2\sqrt{2N_c}} h_{\parallel}^{(t)}(x), \phi_{K^*}^s(x) = \frac{f_{K^*}^T}{2\sqrt{4N_c}} \frac{d}{dx} h_{\parallel}^{(s)}(x), \\ \phi_{K^*}^v(x) &= \frac{f_{K^*}}{2\sqrt{2N_c}} g_{\perp}^{(v)}(x), \phi_{K^*}^a(x) = \frac{f_{K^*}}{8\sqrt{2N_c}} \frac{d}{dx} g_{\perp}^{(a)}(x), \end{aligned} \quad (14)$$

where

$$\phi_{\parallel,\perp} = 6x(1-x) \left[1 + 3a_{1K^*}^{\parallel,\perp} t + 3/2 a_{2K^*}^{\parallel,\perp} (5t^2 - 1) \right], \quad (15)$$

$$h_{\parallel}^{(t)}(x) = 3t^2, \quad h_{\parallel}^{(s)}(x) = 6x(1-x), \quad (16)$$

$$g_{\perp}^{(a)}(x) = 6x(1-x), \quad g_{\perp}^{(v)}(x) = 3/4(1+t^2). \quad (17)$$

The distribution amplitudes of the axial-vectors $a_1(b_1)$ have the same format as those of the K^* meson except for the factor $i\gamma_5$ from the left-hand side:

$$\begin{aligned} & \langle A(P, \epsilon_L^*) | \bar{q}_{2\beta}(z) q_{1\alpha}(0) | 0 \rangle \\ &= \frac{i\gamma_5}{\sqrt{2N_c}} \int_0^1 dx e^{ixp \cdot z} [m_A \epsilon_L^* \phi_A(x) \\ & \quad + \epsilon_L^* \not{P} \phi_A^t(x) + m_A \phi_A^s(x)]_{\alpha\beta}, \\ & \langle A(P, \epsilon_T^*) | \bar{q}_{2\beta}(z) q_{1\alpha}(0) | 0 \rangle \\ &= \frac{i\gamma_5}{\sqrt{2N_c}} \int_0^1 dx e^{ixp \cdot z} [m_A \epsilon_T^* \phi_A^v(x) + \epsilon_T^* \not{P} \phi_A^T(x) \\ & \quad + m_A i \epsilon_{\mu\nu\rho\sigma} \gamma_5 \gamma^\mu \epsilon_T^{*\nu} n^\rho v^\sigma \phi_A^a(x)]_{\alpha\beta}, \end{aligned} \quad (18)$$

where A represents a_1 and b_1 . Their (sub) leading twist wave functions also have the same parameter formats as those of the K^* , which can be obtained by replacing K^* with A in Eq. (14). The corresponding functions $\phi(x)$,

$h(x)$, $g(x)$ for the axial-vector are written as

$$\phi_{\parallel,\perp} = 6x(1-x) \left[a_0^{\parallel,\perp} + 3a_1^{\parallel,\perp} t + \frac{3a_2^{\parallel,\perp}}{2} (5t^2 - 1) \right], \quad (19)$$

$$h_{\parallel}^{(t)}(x) = 3a_0^{\perp} t^2 + \frac{3}{2} a_1^{\perp} t (3t^2 - 1), \quad (20)$$

$$h_{\parallel}^{(s)}(x) = 6x(1-x)(a_0^{\perp} + a_1^{\perp} t), \quad (21)$$

$$g_{\perp}^{(a)}(x) = 6x(1-x)(a_0^{\parallel} + a_1^{\parallel} t), \quad (22)$$

$$g_{\perp}^{(v)}(x) = \frac{3}{4} a_0^{\parallel} (1+t^2) + \frac{3}{2} a_1^{\parallel} t^3, \quad (23)$$

where the zeroth Gegenbauer moments $a_0^{\perp}(a_1) = a_0^{\parallel}(b_1) = 0$ and $a_0^{\parallel}(a_1) = a_0^{\perp}(b_1) = 1$. Here $t = 2x - 1$, and the other decay constants and Gegenbauer moments are listed in Table 1.

Table 1. Decay constants and Gegenbauer moments for K^* , a_1 and b_1 (in MeV). The values are taken at $\mu = 1$ GeV.

f_{K^*}	$f_{K^*}^T$	f_{a_1}	$f_{b_1}^T$
209 ± 2	165 ± 9	238 ± 10	-180 ± 8
$a_1^{\parallel}(K^*)$	$a_1^{\perp}(K^*)$	$a_2^{\parallel}(K^*)$	$a_2^{\perp}(K^*)$
0.03 ± 0.02	0.04 ± 0.03	0.11 ± 0.09	0.10 ± 0.08
$a_2^{\parallel}(a_1(1260))$	$a_2^{\perp}(a_1(1260))$	$a_2^{\parallel}(b_1(1235))$	$a_2^{\perp}(b_1(1235))$
-0.02 ± 0.02	-1.04 ± 0.34	-1.95 ± 0.35	0.03 ± 0.19

The following input parameters are also used in our numerical calculations [18, 19]:

$$f_B = 190 \text{ MeV}, \quad M_B = 5.28 \text{ GeV}, \quad (24)$$

$$\tau_{B\pm} = 1.638 \times 10^{-12} \text{ s}, \quad \tau_{B^0} = 1.525 \times 10^{-12} \text{ s}, \quad (25)$$

$$|V_{ub}| = 3.89 \times 10^{-3}, \quad |V_{tb}| = 1.0, \quad (26)$$

$$|V_{us}| = 0.2252, \quad |V_{ts}| = 38.7 \times 10^{-3}, \quad (27)$$

$$M_W = 80.41 \text{ GeV}, \quad \gamma = (67.2 \pm 3.9)^\circ. \quad (28)$$

First, we use the PQCD approach to calculate the form factors $A_0^{B \rightarrow K^*}$, $V_0^{B \rightarrow a_1}$ and $V_0^{B \rightarrow b_1}$, which are usually the input parameters in other QCD approaches such as QCD factorization (QCDF). For comparison, we list both the results calculated by the PQCD approach and the light-cone sum rules (LCSR) in Table 2, the latter being the input parameters for QCDF calculations. Certainly, our calculations are consistent with previous PQCD calculation results [20].

The decay widths for these channels can be expressed as

$$\Gamma = \frac{G_F^2 (1 - r_{a_1(b_1)}^2 - r_{K^*}^2)}{32\pi M_B} \sum_{L,N,T} M^{\sigma\dagger} M, \quad (29)$$

where $r_{a_1(b_1)} = m_{a_1(b_1)}/M_B$. M^σ is the decay amplitude and can be calculated in the PQCD approach; the subscript σ represents the helicity states of the two final mesons with the longitudinal (L), normal (N) and transverse (T) components. According to Lorentz structure

analysis, the amplitudes are decomposed into

$$M^\sigma = M_B^2 M_L + M_B^2 M_N \epsilon_2^*(\sigma=T) \cdot \epsilon_3^*(\sigma=T) + i M_T \epsilon_{\mu\nu\rho\sigma} \epsilon_2^{\mu*} \epsilon_3^{\nu*} P_2^\rho P_3^\sigma. \quad (30)$$

We can define the longitudinal H_0 and transverse H_\pm helicity amplitudes as

$$H_0 = M_B^2 M_L, \quad (31)$$

$$H_\pm = M_B^2 M_N \mp m_{a_1(b_1)} m_{K^*} \sqrt{\kappa^2 - 1} M_T, \quad (32)$$

where $\kappa = \frac{P_2 \cdot P_3}{m_{a_1(b_1)} m_{K^*}}$. They satisfy the relation

$$\sum_{L,N,T} M^{\sigma\dagger} M = |H_0|^2 + |H_+|^2 + |H_-|^2. \quad (33)$$

When we consider the polarization fractions, another equivalent set of definitions of helicity amplitudes is often used,

$$A_0 = -\zeta M_B^2 M_L, \quad A_\parallel = \zeta \sqrt{2} M_B^2 M_N, \quad A_\perp = \zeta m_{a_1(b_1)} m_{K^*} \sqrt{\kappa^2 - 1} M_T. \quad (34)$$

If the normalization factor satisfying $|A_0|^2 + |A_\parallel|^2 + |A_\perp|^2 = 1$, then $A_0, A_\parallel, A_\perp$ denote the longitudinal, parallel and perpendicular polarization fractions, respectively.

Table 2. Form factors predicted by PQCD approach and light-cone sum rules (LCSR) [21, 22]. The errors in this work include the B meson shape parameter ω_b , the QCD scale $\Lambda_{\text{QCD}}^{(4)}$, the threshold resummation parameter c , and the Gegenbauer moments in K^* or $a_1(b_1)$ meson.

	this work	LCSR
$A_0^{B \rightarrow K^*}(q^2=0)$	$0.30^{+0.04+0.00+0.04+0.00}_{-0.04-0.01-0.04-0.01}$	0.374
$A_1^{B \rightarrow K^*}(q^2=0)$	$0.19^{+0.03+0.01+0.03+0.02}_{-0.02-0.01-0.02-0.01}$	0.292
$V^{B \rightarrow K^*}(q^2=0)$	$0.25^{+0.05+0.01+0.03+0.03}_{-0.03-0.02-0.02-0.01}$	0.411
$V_0^{B \rightarrow a_1}(q^2=0)$	$0.33^{+0.05+0.01+0.08+0.11}_{-0.04-0.01-0.07-0.09}$	0.30 ± 0.05
$V_1^{B \rightarrow a_1}(q^2=0)$	$0.30^{+0.06+0.03+0.10+0.08}_{-0.04-0.04-0.09-0.08}$	0.37 ± 0.07
$A^{B \rightarrow a_1}(q^2=0)$	$0.23^{+0.05+0.03+0.04+0.05}_{-0.03-0.01-0.04-0.05}$	0.48 ± 0.09
$V_0^{B \rightarrow b_1}(q^2=0)$	$0.44^{+0.06+0.00+0.07+0.04}_{-0.05-0.01-0.06-0.04}$	-0.39 ± 0.07
$V_1^{B \rightarrow b_1}(q^2=0)$	$0.29^{+0.05+0.01+0.06+0.03}_{-0.03-0.01-0.05-0.04}$	-0.20 ± 0.04
$A^{B \rightarrow b_1}(q^2=0)$	$0.19^{+0.04+0.00+0.04+0.03}_{-0.02-0.01-0.04-0.03}$	-0.25 ± 0.05

Using the input parameters as specified in this section, it is easy to get the branching ratios for the decays considered. The results are listed in Table 3, where the first error comes from the uncertainty in the B meson shape parameter $\omega_b = 0.40 \pm 0.04$ GeV, the second error is induced by the hard scale-dependent variation from $\Lambda_{\text{QCD}}^{(4)} = 0.25 \pm 0.05$, the third is from the threshold resummation parameter c varying from 0.3 to 0.4, and the last error is from the Gegenbauer moments in K^* and $a_1(b_1)$ mesons.

Table 3. Branching ratios (in units of 10^{-6}) for the decays $B \rightarrow a_1(1260)K^*$ and $B \rightarrow b_1(1235)K^*$. In our results, the errors for these entries correspond to the uncertainties from $\omega_b, \Lambda_{\text{QCD}}^{(4)}$, the threshold resummation parameter c , and the Gegenbauer moments in the final state mesons, respectively. For comparison, we also list the results predicted by the QCDF approach [7] and the naive factorization approach [8].

	this work	[7]	[8]
$\bar{B}^0 \rightarrow a_1^+ K^{*-}$	$9.9^{+1.6+0.4+3.7+6.2}_{-1.1-0.6-3.7-4.2}$	$10.6^{+5.7+31.7}_{-4.0-8.1}$	0.92
$\bar{B}^0 \rightarrow a_1^0 \bar{K}^{*0}$	$7.1^{+1.5+0.4+3.1+4.0}_{-0.9-0.6-3.1-3.5}$	$4.2^{+2.8+15.5}_{-1.9-4.2}$	0.64
$B^- \rightarrow a_1^- \bar{K}^{*0}$	$10.8^{+2.0+0.7+4.6+7.1}_{-1.4-0.8-4.6-4.7}$	$11.2^{+6.1+31.9}_{-4.4-9.0}$	0.51
$B^- \rightarrow a_1^0 K^{*-}$	$4.8^{+0.6+0.2+1.6+3.0}_{-0.5-0.3-1.6-2.1}$	$7.8^{+3.2+16.3}_{-2.5-4.3}$	0.86
$\bar{B}^0 \rightarrow b_1^+ K^{*-}$	$18.0^{+3.3+1.3+6.3+3.5}_{-2.6-2.3-6.3-3.2}$	$12.5^{+4.7+20.1}_{-3.7-9.0}$	0.32
$\bar{B}^0 \rightarrow b_1^0 \bar{K}^{*0}$	$9.6^{+2.1+1.0+3.8+1.9}_{-1.5-1.1-3.8-1.6}$	$6.4^{+2.4+8.8}_{-1.7-4.8}$	0.15
$B^- \rightarrow b_1^- \bar{K}^{*0}$	$23.0^{+4.5+2.3+8.4+4.5}_{-3.5-2.9-8.4-4.1}$	$12.8^{+5.0+20.1}_{-3.8-9.6}$	0.18
$B^- \rightarrow b_1^0 K^{*-}$	$10.6^{+1.9+0.7+3.4+4.2}_{-1.5-1.4-3.4-2.0}$	$7.0^{+2.6+12.0}_{-2.0-4.8}$	0.12

In our predictions, the branching ratio of the decay $\bar{B}^0 \rightarrow a_1^0 \bar{K}^{*0}$ is larger than that of the decay $B^- \rightarrow a_1^0 K^{*-}$. This is mainly due to the amplitudes of the factorizable emission diagrams, F_{ea_1} and F_{eK^*} , having opposite interference effects for these two decays: constructive for the decay $a_1^0 \bar{K}^{*0}$, destructive for the decay $a_1^0 K^{*-}$. The decay $\bar{B}^0 \rightarrow a_1^0 \bar{K}^{*0}$ therefore receives a larger real part for the penguin amplitudes. Though the decay $B^- \rightarrow a_1^0 K^{*-}$ has much larger contributions from tree amplitudes, these are CKM suppressed and cannot change the branching ratio too much. In order to characterize the contributions from tree operators and the symmetry breaking effects between B^- and \bar{B}^0 mesons, it is useful to define two ratios:

$$R_1 = \frac{\mathcal{B}(B^- \rightarrow a_1^- \bar{K}^{*0})}{\mathcal{B}(\bar{B}^0 \rightarrow a_1^+ K^{*-})} \times \frac{\tau_{\bar{B}^0}}{\tau_{B^-}}, \quad (35)$$

$$R_2 = \frac{\mathcal{B}(B^- \rightarrow b_1^0 K^{*-})}{\mathcal{B}(\bar{B}^0 \rightarrow b_1^+ K^{*-})} \times \frac{\tau_{\bar{B}^0}}{\tau_{B^-}}. \quad (36)$$

If one neglects the tree operators and the electro-weak penguins, the ratios obey the following limits

$$R_1 = 1, \quad R_2 = 0.5. \quad (37)$$

Here our predictions for these two ratios are 1.02 and 0.55, respectively. The results predicted by the QCDF approach are 0.98 and 0.52, respectively. If the future data for R_1 show a large deviation from our value, the contributions from electro-weak penguin operators might have an important effect, as the contributions from tree operators cannot change the branching ratio of $\bar{B}^0 \rightarrow a_1^+ K^{*-}$ too much. If the future data for R_2 have a large deviation from our value, some mechanism beyond factorization, or even new physics, might have an important effect, because the factorization formulae for

$\bar{B}^0 \rightarrow b_1^+ K^{*-}$ and $B^- \rightarrow b_1^0 K^{*-}$ are exactly the same if the neutral b_1^0 meson decay constant vanishes.

Table 3 shows that, when compared with other results, our predictions are consistent with the QCDF results within (large) theoretical errors, while in stark disagreement with the naive factorization approach, where the nonfactorizable effects are described by the effective number of colors N_c^{eff} . For some decays, where the contributions from the emission diagrams are dominant or the branching ratios have a strong dependence on the correlative form factors, the naive factorization approach can give a reasonable prediction, while for decays where the annihilation diagrams play an important role, this approach shows some disadvantages. On the experimental side, BarBar has searched for the decays $B \rightarrow a_1^- \bar{K}^{*0}$, $b_1 K^*$ and set upper limits on their branching ratios ranging from 3.3 to 8.0×10^{-6} at the 90% confidence level [9, 10]. These upper limits are obtained, however, by assuming that $\mathcal{B}(a_1^\pm \rightarrow \pi^+ \pi^- \pi^\pm) = \mathcal{B}(a_1^\pm \rightarrow \pi^0 \pi^0 \pi^\pm)$ and $\mathcal{B}(a_1^\pm (b_1^\pm) \rightarrow \rho^0 (\omega) \pi^\pm) = 1$. Furthermore, the background signals may have an important effect on these upper limits, such as the background decay channel $B \rightarrow a_2 \bar{K}^{*0}$ in studies of the decay $B \rightarrow a_1 \bar{K}^{*0}$. In view of these disagreements, we strongly suggest that LHCb and the forthcoming Super-B experiments accurately measure these decay modes.

From Table 4, we find that the polarization characteristics for the decays $B \rightarrow a_1 K^*$ and $B \rightarrow b_1 K^*$ are very different: the transverse polarization amplitudes have almost equal values with (even a little stronger than) the longitudinal polarization amplitudes for the former, while the longitudinal polarization states are dominant for the latter. It seems that the anomalous polarizations which occur in $B \rightarrow \phi K^*$, ρK^* decays also happen in $B \rightarrow a_1 K^*$ decays, while they do not occur in $B \rightarrow b_1 K^*$ decays. We also find that the contributions from the annihilation diagrams are very important for the final polarization fractions for $B \rightarrow a_1 K^*$ decays: if these contributions are neglected, the longitudinal polarization fraction of the decay $B^- \rightarrow a_1^0 K^{*-}$ becomes 98.8%, those of

$\bar{B}^0 \rightarrow a_1^+ K^{*-}$, $a_1^0 \bar{K}^{*0}$ increase to about 90%, and that of the decay $B^- \rightarrow a_1^- \bar{K}^{*0}$ changes from 50.3% to 70.0%. The longitudinal polarizations of $B \rightarrow b_1 K^*$ decays decrease very little if the annihilation type contributions are neglected, except for the decay $B^- \rightarrow b_1^- \bar{K}^{*0}$, which has a larger reduction, changing from 96.2% to 86%. In short, compared to $B \rightarrow a_1 K^*$ decays, the longitudinal polarizations of $B \rightarrow b_1 K^*$ decays are not very sensitive to the annihilation type contributions.

Now we turn to evaluations of the CP -violating asymmetries in the PQCD approach. Here we only research the decays $B \rightarrow b_1 K^*$, where the transverse polarization fractions are very small and range from 3.8 to 5.2%. It is easy to see that for these $b_1 K^*$ decay modes, the contributions from the transverse polarizations are very small, so we neglect them in our calculations. Consider these two matrix elements

$$\begin{aligned} M_L &= V_{ub} V_{us}^* T_L - V_{tb} V_{ts}^* P_L \\ &= V_{ub} V_{us}^* T_j (1 + z_j e^{i(\gamma + \delta_j)}), \end{aligned} \quad (38)$$

$$\begin{aligned} \bar{M}_L &= V_{ub}^* V_{us} T_L - V_{tb}^* V_{ts} P_L \\ &= V_{ub}^* V_{us} T_L (1 + z_L e^{i(-\gamma + \delta_L)}), \end{aligned} \quad (39)$$

where γ is the CKM weak phase angle, defined via $\gamma = \arg \left[-\frac{V_{tb} V_{ts}^*}{V_{ub} V_{us}^*} \right]$; δ_L is the relative strong phase between the tree and the penguin amplitudes, which are denoted as ‘ T_L ’ and ‘ P_L ’, respectively; and the term z_L describes the ratio of penguin to tree contributions and is defined as

$$z_L = \left| \frac{V_{tb} V_{ts}^*}{V_{ub} V_{us}^*} \right| \left| \frac{P_L}{T_L} \right|. \quad (40)$$

Using Eq. (38) and Eq. (39), one can get the expression for the direct CP -violating asymmetry:

$$\begin{aligned} \mathcal{A}_{CP}^{\text{dir}} &= \frac{|\bar{M}|^2 - |M|^2}{|M|^2 + |\bar{M}|^2} \\ &= \frac{2z_L \sin \gamma \sin \delta_L}{(1 + 2z_L \cos \gamma \cos \delta_L + z_L^2)}. \end{aligned} \quad (41)$$

Table 4. Longitudinal polarization fraction (f_L) and two transverse polarization fractions (f_{\parallel} , f_{\perp}) for decays $B \rightarrow a_1(1260)K^*$ and $B \rightarrow b_1(1235)K^*$. In our results, the uncertainties are the same as those in Table 3. For comparison, the results of f_L as predicted by the QCDF approach are displayed in parentheses.

	f_L (%)	f_{\parallel} (%)	f_{\perp} (%)
$\bar{B}^0 \rightarrow a_1^+ K^{*-}$	$48.9^{+5.1+7.4+4.9+8.8}_{-4.7-8.0-4.9-7.2}$ (37 ⁺³⁹ ₋₂₉)	$26.1^{+2.5+3.8+2.6+3.2}_{-2.8-4.1-2.6-3.1}$	$25.0^{+2.2+3.8+2.3+2.8}_{-2.3-3.5-2.3-2.8}$
$\bar{B}^0 \rightarrow a_1^0 \bar{K}^{*0}$	$59.6^{+4.7+7.7+4.3+4.5}_{-4.9-7.8-4.3-5.1}$ (23 ⁺⁴⁵ ₋₁₉)	$20.2^{+2.6+3.8+2.2+0.1}_{-2.5-3.8-2.2-2.2}$	$20.2^{+2.3+4.0+2.1+0.2}_{-2.2-3.5-2.1-2.1}$
$B^- \rightarrow a_1^- \bar{K}^{*0}$	$50.3^{+5.1+8.6+5.0+7.4}_{-4.9-9.9-5.0-8.6}$ (37 ⁺⁴⁸ ₋₃₇)	$24.1^{+2.6+5.0+2.5+3.9}_{-2.7-3.7-2.5-3.5}$	$25.6^{+2.3+5.0+2.5+4.7}_{-2.4-4.9-2.5-3.9}$
$B^- \rightarrow a_1^0 K^{*-}$	$49.0^{+3.3+6.2+4.7+5.9}_{-4.3-6.2-4.7-5.1}$ (52 ⁺⁴¹ ₋₄₂)	$25.5^{+2.3+0.0+2.4+2.5}_{-2.5-2.5-2.4-2.9}$	$25.5^{+2.0+3.2+2.2+2.6}_{-2.2-3.7-2.2-3.0}$
$\bar{B}^0 \rightarrow b_1^+ K^{*-}$	$95.9^{+0.1+1.1+0.0+0.6}_{-0.1-1.3-0.0-1.3}$ (82 ⁺¹⁸ ₋₄₁)	$1.1^{+0.2+0.4+0.2+0.4}_{-0.0-0.2-0.2-0.3}$	$3.0^{+0.0+0.9+0.2+0.4}_{-0.1-0.7-0.2-0.6}$
$\bar{B}^0 \rightarrow b_1^0 \bar{K}^{*0}$	$95.4^{+0.1+1.0+0.1+0.4}_{-0.1-1.4-0.1-1.3}$ (79 ⁺²¹ ₋₇₄)	$0.9^{+0.0+0.2+0.4+0.2}_{-0.0-0.2-0.4-0.3}$	$3.7^{+0.1+1.2+0.3-0.5}_{-0.1-0.8-0.3-0.9}$
$B^- \rightarrow b_1^- \bar{K}^{*0}$	$96.2^{+0.0+0.9+0.1+0.6}_{-0.0-1.7-0.1-0.7}$ (79 ⁺²¹ ₋₇₄)	$1.0^{+0.0+0.3+0.3+0.2}_{-0.0-0.3-0.3-0.4}$	$2.8^{+0.0+0.9+0.2+0.4}_{-0.0-0.6-0.2-0.5}$
$B^- \rightarrow b_1^0 K^{*-}$	$96.5^{+0.0+0.8+0.1+0.2}_{-0.1-1.3-0.1-0.8}$ (82 ⁺¹⁶ ₋₂₆)	$0.7^{+0.1+0.2+0.2+0.3}_{-0.0-0.1-0.2-0.2}$	$2.8^{+0.0+0.9+0.3+0.3}_{-0.0-0.6-0.3-0.4}$

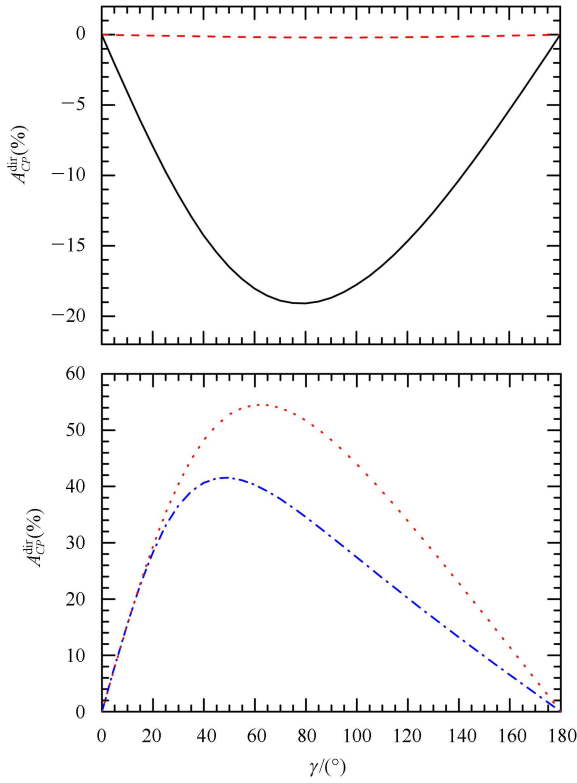


Fig. 1. Direct CP -violating asymmetry as a function of CKM angle γ . The dashed line is for the decay $B^- \rightarrow b_1^- \bar{K}^{*0}$, the solid line represents the decay $\bar{B}^0 \rightarrow b_1^+ \bar{K}^{*0}$, the dotted line represents the decay $B^- \rightarrow b_1^0 \bar{K}^{*-}$, and the dot-dashed line is for the decay $\bar{B}^0 \rightarrow b_1^+ K^{*-}$.

Note that the contributions from the transverse polarizations have been neglected in the derivation of the direct CP -violating asymmetry.

Using the input parameters and the wave functions as specified in this section, one can find the PQCD predictions (in units of 10^{-2}) for the direct CP -violating asymmetries of the decays considered:

$$\mathcal{A}_{CP}^{\text{dir}}(\bar{B}^0 \rightarrow b_1^+ K^{*-}) = 38.5_{-1.7-7.4-4.5-1.3}^{+1.2+8.8+4.5+0.8}, \quad (42)$$

$$\mathcal{A}_{CP}^{\text{dir}}(B^- \rightarrow b_1^0 K^{*-}) = 54.3_{-1.7-6.7-4.4-2.2}^{+0.9+7.8+4.4+1.2}, \quad (43)$$

$$\mathcal{A}_{CP}^{\text{dir}}(\bar{B}^0 \rightarrow b_1^0 \bar{K}^{*0}) = -18.7_{-1.3-0.3-1.8-1.4}^{+2.0+0.7+1.8+1.6}, \quad (44)$$

$$\mathcal{A}_{CP}^{\text{dir}}(B^- \rightarrow b_1^- \bar{K}^{*0}) = -0.18_{-0.28-0.00-0.33-0.11}^{+0.23+0.47+0.33+0.11}, \quad (45)$$

where the errors are induced by the uncertainties in the B meson shape parameter $\omega_b = 0.4 \pm 0.04$, the hard scale-

dependent variation from $\Lambda_{\text{QCD}}^{(4)} = 0.25 \pm 0.05$, the threshold resummation parameter c varying from 0.3 to 0.4, and the Gegenbauer moments in the final state mesons. In Fig. 1, we show the CKM angle γ dependence of the direct CP -violating asymmetries for the four decays above. It is particularly noteworthy that our predictions about the direct CP asymmetries of these decays are consistent with the QCDF results [23]:

$$\mathcal{A}_{CP}^{\text{dir}}(\bar{B}^0 \rightarrow b_1^+ K^{*-}) = (44_{-58}^{+3})\%, \quad (46)$$

$$\mathcal{A}_{CP}^{\text{dir}}(B^- \rightarrow b_1^0 K^{*-}) = (60_{-73}^{+6})\%, \quad (47)$$

$$\mathcal{A}_{CP}^{\text{dir}}(\bar{B}^0 \rightarrow b_1^0 \bar{K}^{*0}) = (-17_{-10}^{+21})\%, \quad (48)$$

$$\mathcal{A}_{CP}^{\text{dir}}(B^- \rightarrow b_1^- \bar{K}^{*0}) = (2_{-2}^{+0})\%, \quad (49)$$

where the error comes from the parameters $\rho_{A,H}$ and arbitrary phases $\phi_{A,H}$. These are phenomenological parameters to cure the endpoint divergences in the amplitudes for the annihilation and hard spectator scattering diagrams.

4 Conclusion

In this paper, by using the decay constants and light-cone distribution amplitudes derived from the QCD sum-rule method, we studied the $B \rightarrow a_1 K^*$, $b_1 K^*$ decays in the PQCD factorization approach and found that:

1) Our predictions for the branching ratios are consistent with the QCDF results within errors, but larger than the values calculated by the naive factorization approach. On the experimental side, some primary upper limit values are inexplicable. In view of these disagreements, we strongly suggest that LHCb and the forthcoming Super-B experiments perform further studies to accurately measure these decay modes.

2) The anomalous polarizations which occur in $B \rightarrow \phi K^*$, ρK^* decays also happen in $B \rightarrow a_1 K^*$ decays, but not in $B \rightarrow b_1 K^*$ decays. Here, the contributions from the annihilation diagrams play an important role in explaining the larger transverse polarizations in the $B \rightarrow a_1 K^*$ decays, while they are not sensitive to the polarizations in $B \rightarrow b_1 K^*$ decays.

3) Our predictions for the direct CP -asymmetries agree well with the QCDF results, within errors. The decays $\bar{B}^0 \rightarrow b_1^+ K^{*-}$, $B^- \rightarrow b_1^0 K^{*-}$ have larger direct CP -asymmetries, which could be measured by the present LHCb and the forthcoming Super-B experiments.

References

- 1 LI Ying, LU Cai-Dian. Phys. Rev. D, 2006, **73**: 014024
- 2 HUANG Han-Wen, LÜ Cai-Dian, Morii T et al. Phys. Rev. D, 2006, **73**: 014011
- 3 Ali A, Kramer G, LI Ying et al. Phys. Rev. D, 2007, **76**: 074018
- 4 Beneke M, Rohrer J, YANG De-Shan. Phys. Lett. B, 2007, **768**: 51
- 5 Barberio E et al. (Heavy Flavor Averaging Group). arXiv: hepex/0808.1297 and online update <http://www.slac.stanford.edu/xorg/hfag>.
- 6 Aubert B et al. (BABAR collaboration). Phys. Rev. Lett., 2006, **97**: 201801
- 7 CHENG Hai-Yang, YANG Kwei-Chou. Phys. Rev. D, 2008, **78**: 094001
- 8 Calderon G, Munoz J H, Vera C E. Phys. Rev. D, 2007, **76**: 094019
- 9 Aubert B et al. (BABAR collaboration). Phys. Rev. D, 2010, **82**: 091101
- 10 Aubert B et al. (BABAR collaboration). Phys. Rev. D, 2009, **80**: 051101
- 11 Keum Y Y, LI Hsiang-nan, Sanda A I. Phys. Lett. B, 2001, **504**: 6; Phys. Rev. D, 2001 **63**: 054008; LÜ Cai-Dian, Ukai K, YANG Mao-Zhi. Phys. Rev. D, 2001, **63**: 074009; Keum Y Y, Li Hsiang-nan. Phys. Rev. D, **63**: 2001, 074006; LÜ Cai-Dian, YANG Mao-Zhi. Eur. Phys. J. C, 2002, **23**: 275
- 12 Li Hsiang-nan, Mishima S, Sanda A I. Phys. Rev. D, 2005, **72**: 114005
- 13 Li Hsiang-nan, Tseng B. Phys. Rev. D, 1998, **57**: 443
- 14 Li Hsiang-nan, Ukai K. Phys. Lett. B, 2003, **555**: 197
- 15 Li Hsiang-nan, YU Hoi-Lai. Phys. Rev. D, 1996, **53**: 2480
- 16 Buchalla G, Buras A J, Lautenbacher M E. Rev. Mod. Phys., 1996, **68**: 1125
- 17 LÜ Cai-Dian, YANG Mao-Zhi. Eur. Phys. J. C, 2003, **28**: 515
- 18 Nakamura K et al. (Particle Data Group). J. Phys. G, 2010, **37**: 48
- 19 CKMfitter Group. <http://ckmfitter.in2p3.fr>
- 20 LI Run-Hui, LU Cai-Dian, WANG Wei. Phys. Rev. D, 2009, **79**: 034014
- 21 Ball P, Zwicky R. Phys. Rev. D, 2005, **71**: 014029
- 22 YANG Kwei-Chou. Phys. Rev. D, 2008, **78**: 034018
- 23 YANG Kwei-Chou. arXiv:hep-ph/0810.1782